Technology Brief

Multi-Normalization and Interpolation Protocol to Improve Norovirus Immunoagglutination Assay from Paper Microfluidics with Smartphone Detection

Authors:

Soohee Cho[1], Tu San Park[1†], Kelly A. Reynolds[2] and Jeong-Yeol Yoon[1,3]

Affiliations:

[1]Department of Agricultural and Biosystems Engineering, and [2]Mel and Enid Zuckerman College of Public Health, [3]Department of Biomedical Engineering, The University of Arizona, Tucson, Arizona 85721, USA

[†]Present address: Department of Bio-industrial Machinery Engineering, Kyungpook National University, Daegu 750-701, Republic of Korea.

Corresponding Author:

Jeong-Yeol Yoon, Department of Biomedical Engineering and Department of Agricultural and Biosystems Engineering, The University of Arizona, 1177 E. 4th St., Rm. 403, Tucson, AZ 85721-0038, USA. E-mail: jyyoon@email.arizona.edu.

Abstract

Norovirus (NoV) is one of the leading causes of acute gastroenteritis, affecting 685 million people per year around the world. The best preventive measure is to screen water for possible NoV contamination, not from infected humans, preferably utilizing rapid and field-deployable diagnostic methods. While enzyme immunoassays (EIAs) can be used for such detection, the low infectious dose as well as the generally inferior sensitivity and low titer of available NoV antibodies render critical challenges in using EIAs towards NoV assays. In this work, we demonstrated smartphone-based Mie scatter detection of NoV with immunoagglutinated latex particles on paper microfluidic chips. Using only three different concentrations of anti-NoV conjugated particles, we were able to construct a single standard curve that covered seven orders of magnitude of NoV antigen concentrations. Multiple normalization steps and interpolation procedures were developed to estimate the optimum amount of antibody-conjugated particles that matched to the target NoV concentration. We also demonstrated a very low detection limit of 10 pg/mL without using any concentration or enrichment steps. This method can also be adapted to any other virus pathogens whose antibodies possess low sensitivity and low antibody titer.

Keywords: Paper microfluidic analytic device; µPAD; smartphone; biosensor; water safety

INTRODUCTION

Norovirus (NoV) is the leading cause of illness and outbreaks from contaminated food and water around the world. According to the U.S. Centers for Disease Control and Prevention (CDC), NoV causes 19-21 million cases of acute gastroenteritis annually in the United States, and 685 million cases globally. NoV is extremely contagious with an infectious dose as few as 18 viral particles[1] or $1x10^2$ copies/mL.[2]

The standard diagnostic methods are: 1) detection of viral RNA by reverse transcription-polymerase chain reaction (RT-PCR) or 2) detection of viral antigens by enzyme immunoassays (EIAs), including enzyme-linked immunosorbent assay (ELISA). While RT-PCR provides excellent sensitivity with a detection limit of $<10^2$ copies/mL,[3] this technique is time-consuming, laborious, and requires expensive equipment and reagents that may not be readily available. Although EIAs are inferior to RT-PCR in their sensitivity and detection limits, they provide rapid results and serve as a preliminary detection method to meet acute gastroenteritis outbreak analysis demands. Thus, many commercial EIA kits are available. For example, RIDASCREEN® Norovirus 3rd Generation EIA has been cleared by the U.S. Food and Drug Administration (FDA). However, its intended use is limited to NoV detection in human stool from ill patients (thus not requiring low detection limit) and RT-PCR validation is still recommended. To be used as a preventive measure especially for water samples, high sensitivity and very low detection limit are necessary. Unfortunately, most antibodies to NoV show low reactivity with specific NoV strains, leading to a very high detection limit (i.e. > 10^6 virus particles per gram of feces).[4] In addition, most currently available NoV antibodies have a significantly low antibody titer (or ELISA titer). This leads to an extremely narrow linear range of detection, thus rendering the assay less useful for NoV

quantification. All of these complications are more or less associated with the uncultivable nature of NoV.[5]

Due to these limitations, NoV has been detected from stool samples from progressively ill human subjects, where NoV concentrations are very high. To develop preventive diagnostic tool for acute gastroenteritis outbreaks, potentially contaminated water sources must be tested. Towards this end, there is a need to improve NoV EIAs towards: 1) very low detection limit and 2) a much wider concentration range, enabling rapid, sensitive, and easily quantifiable assays. There have been several recent studies to improve NoV EIAs through alternative sensing modalities or sample enrichment (i.e. concentration methods). These recent studies are summarized in **Table 1**, where detection limits were indeed reduced by various means. However, these methods require additional steps that are complicated and time-consuming, including sample purification/enrichment,[2,6,7] use of NoV virus-like particles (VLPs),[7-11] or the use of RT-PCR,[11] thus forgoing the true merits of EIAs over RT-PCR.

Our group has previously demonstrated particle immunoagglutination assay coupled with angle-specific Mie scatter detection on various microfluidic platforms for assaying various pathogens.[12-17] In this assay, antibody-conjugated latex particles immunologically agglutinate in the presence of target antigens, thus increasing the effective particle diameter. Monitoring Mie scatter at an angle optimized for such agglutination allows the detection and quantification of target antigens. Additionally, particle immunoagglutination has been demonstrated on simple and low-cost paper microfluidic platforms.[14,15] More importantly, paper platforms provide an additional advantage in providing intrinsic filtration capabilities with the fibrous pores, as

previously demonstrated.[18] Incorporating smartphone-based detection with paper microfluidics has allowed momentous strides towards field-deployable, affordable, and easy-to-use assays.[17]

Our previous studies demonstrated low detection limits using Mie scatter detection of immunoagglutinated latex particles on paper microfluidic platforms. This principle worked successfully with commercially available antibodies that have high ELISA titer, e.g., 1 : 17,000 of antibody to *Escherichia coli* (anti-*E. coli*). However, such methods are limited with low ELISA titer antibodies, such as anti-NoV (1 : 2,000). In fact, preliminary studies performed in our laboratory showed a mere one order of magnitude linear range for a Mie scatter immunoagglutination NoV assay.

In this work, we demonstrated a particle immunoagglutination assay of the capsid proteins from NoV using smartphone-based Mie scatter detection. Wax printing was used as a simpler means for fabricating paper microfluidic channels, which has recently gained wide popularity in the microfluidics area.[19-21] Capsid proteins from the viral coat of NoV were used as a realistic surrogate without risking use of actual infectious samples. Positive signals were normalized following previously performed methods.[15] Three different concentrations of anti-NoV conjugated latex particles were introduced to three different channels of a single paper microfluidic chip. Through interpolation analysis, we demonstrated the linear range of assay over seven orders of magnitude, which has not been demonstrated previously. In addition, we also demonstrated extremely low detection limits, down to 10 pg/mL, which has not yet been demonstrated for NoV EIAs in a rapid assay platform. Such enhancements in sensitivity and broad assay range will provide a strong promise for the EIAs with weak antibodies, towards efficiently determining the contamination source and preventing epidemics.

MATERIALS AND METHOD

Fabrication of Paper Microfluidic Chips

Fabrication of paper microfluidic chips using a wax printer is demonstrated in **Fig. 1**. Paper microfluidic chips with multiple parallel channels were loaded with different amounts of antibody conjugated or bovine serum albumin (BSA) conjugated latex particles. Chips were designed using SolidWorks (Dassault Systemes, SolidWorks Corporation; Waltham, MA, USA) with inlet and absorbent pad dimensions of 4-mm wide and 2-mm long, and channel dimensions of 2-mm wide and 14.5-mm long. Chip designs were printed with solid ink on cellulose chromatography paper (GE Healthcare, Maidstone, Kent, UK) using a wax printer (ColorQube 8580, Xerox, Wilsonville, OR, USA). Individual chips were cut out and placed on a hot plate at 100°C for < 100 seconds to melt the wax through the entire paper. Chips were stored in sealed, dry, and dark conditions if not used immediately.

Conjugation of Anti-NoV to Latex Particles

Polystyrene (PS) latex particles (Magsphere, Pasadena, CA, USA) of 920-nm diameter were covalently conjugated with polyclonal antibodies to norovirus capsid protein (anti-NoV; Abcam, Cambridge, MA, USA) or bovine serum albumin (BSA; Sigma-Aldrich) following the protocol described in Cho et al.[15] The concentrations of conjugated particle suspensions were calibrated by the method detailed in Park et al.[17] and You et al.[12] to yield varying particle concentrations (w/v %) from 0.01%, 0.022%, and 0.045%, for both anti-NoV conjugated particles and BSA conjugated particles. These particles were stored in deionized (DI) water at 4°C.

Sample Preparation

Positive samples consisted of recombinant NoV capsid protein antigens (MyBioSource, San Diego, CA, USA) diluted in sterilized DI water. Dilutions were made to the following concentrations: 10 pg/mL, 100 pg/mL, 1 ng/mL, 10 ng/mL, 100 ng/mL, 1 μg/mL, and 10 μg/mL. DI water without the presence of NoV antigens was used as a blank sample.

Smartphone-based Immunoassay Procedure

A smartphone (iPhone 5, Apple, Cupertino, CA, USA) was positioned in a 3D-printed angled holder described in Cho et al.[15] The smartphone was angled 25° and 9 cm vertically from the paper microfluidic chip (**Fig. 1c**), where the Mie scatter simulation showed the greatest change in scattering intensity as the particle size increased. The smartphone app VSCO (Visual Supply Company, Oakland, CA, USA) was used to lock white balance and focus to the channel center, and images were taken with a shutter speed of 1/600 s on average (**Fig. 1c**). All experiments were performed under a normal ambient lighting condition (fluorescent lamps).

A volume of 1.7 μL of anti-NoV conjugated particles or BSA conjugated particles was pre-loaded on the center of each positive channel or negative channel, respectively. Paper chips were subsequently dried at room temperature. 7 μL of sample (with varying NoV concentration) was added to the positive channel (with anti-NoV conjugated particles pre-loaded), as well as the negative channel (with BSA conjugated particles pre-loaded). Identical particle concentrations (anti-NoV or BSA conjugated) were used when comparing the positive to the negative channel results.

Two image acquisitions were performed for normalization purposes. The first image was taken after the pre-loaded particles were dried (**Fig. 1c**). The second image was taken after the loaded samples entered the absorbent pad (**Fig. 1d**). Triplicate sets of experiments were performed for each particle concentration (a total of 3 concentrations) and each target NoV concentration (a total of 8 concentrations including a blank) - each time using a new microfluidic chip with different samples.

The extent of particle immunoagglutination was measured at the channel center. RGB images were split into their green channel components using ImageJ software (National Institute of Health; Bethesda, MD, USA). Scatter intensities were recorded from the microfluidic channel centers in these green channel images, which have previously enabled maximum change in scatter intensity under ambient lighting.[18] Upon immunoagglutination, the effective size of particles is expected to increase, causing an increase in scatter intensity at the optimized detection angle. This increase can be quantified from the (green) pixel intensities taken from the central area of each channel. A sample intensity plot is shown in **Fig. 1d**, where the channel pre-loaded with 0.01 w/v% anti-NoV particles shows the maximum pixel intensities with 1 ng/mL NoV sample.

Data Normalization

After obtaining signal intensities, double-normalization was done similar to the previously detailed method in Cho et al.[15] The first step is “background-normalization” by dividing the green scatter intensity from the central channel region with that from the background. This step accounts for the channel-to-channel variation and the effects of different ambient lighting

conditions of individual channels. The second step is “blank-normalization” by dividing the background normalized value from the positive channel (pre-loaded with anti-NoV conjugated particles) with the same from the negative channel (pre-loaded with BSA conjugated particles). All channels were loaded with the same amount of anti-NoV and BSA conjugated particles. This step accounts for any variations arising from the extent of non-specific aggregation of anti-NoV particles, in reference to the non-aggregated BSA conjugated particles, prior to performing immunoagglutination assays.

Construction of Standard Curve through Data Interpolation

After double normalization, three double-normalized intensities per particle concentration were available for each NoV concentration. An equivalent amount of antibody conjugated particles was obtained for each NoV concentration through interpolating these raw data, which is described in Results and Discussion. This equivalent amount of antibody conjugated particles was plotted against NoV concentration to construct a standard curve. Analysis of variance (ANOVA) of this standard curve was performed by Stata/IC 12.0.[22]

RESULTS AND DISCUSSION

Double-normalized intensities were obtained from the particle immunoagglutination assays on the paper microfluidic chips using a smartphone. **Fig. 2a** shows the results of NoV assays with varying concentrations of pre-loaded anti-NoV particles. While seven orders of magnitude of NoV concentrations were evaluated in this work, the linear range of assay appeared limited, covering just a few orders of magnitude followed by a decrease in double normalized

scatter intensities, for the given amount of anti-NoV conjugated particles. This can be explained by the inferior sensitivity and very low ELISA titer of anti-NoV used in this study.

However, a noticeable trend can be observed from the entire data set. It is possible to find out the optimum anti-NoV particle concentration for detecting specific NoV concentration through stacking the three individual plots (**Fig. 2b**). For 10^1 pg/mL, the double-normalized intensity was maximized with 0.01% anti-NoV particles. This maximum intensity seemed to gradually shift to the channel with 0.022% anti-NoV particles as NoV concentration increased up to 10 ng/mL (= 10^4 pg/mL). Further shift was observed with the 0.045% anti-NoV particles as NoV concentration increased to 1 μg/mL (= 10^6 pg/mL) and 10 μg/mL (= 10^7 pg/mL). Apparently, an optimum amount of anti-NoV conjugated particles, and thus an antibody amount, seemed to exist for the given concentration of NoV capsid proteins. Such antibody amounts were calculated through interpolating the raw data set shown in **Fig. 2**.

The interpolated value of anti-NoV conjugated particles for the given NoV concentration was calculated in the following manner (**Fig. 3**): First, three double-normalized intensities were divided by the lowest double-normalized intensities (i.e. normalization to the minimum intensity), then multiplied by 100. Second, these intensities were divided by the sum of all intensities obtained in the first step. For example, the 10 pg/mL data can be represented as 60% with the 0.01% anti-NoV particles, 40% with the 0.022% anti-NoV particles, and 0% with the 0.045% anti-NoV particles (the last is the minimum intensity). Therefore, the matching amount of anti-NoV particles should be in between 0.01% and 0.022%, with 60% close to 0.01% and 40% close to 0.022%. To obtain the interpolated amount of anti-NoV particles, the particle concentration was multiplied with the rendered percentage and added together, e.g. 0.01% × 0.6 + 0.022% × 0.4 =

0.015% for the 10 pg/mL data set. This number indicates the estimated particle concentration that optimally matches to the given NoV concentration. Through repeating this calculation for individual trials, it is also possible to obtain standard errors for the estimated particle concentrations.

The interpolated anti-NoV particle concentrations were plotted against the NoV concentrations to construct a single standard curve, and the result is shown in **Fig. 4**. The curve yielded a generally increasing trend, with a linear equation of $y = 0.0052x + 0.0043$ and R^2 value of 0.94. This linear equation can be used to determine NoV concentration from three double normalized intensities from a single chip. A positive correlation between the anti-NoV particle concentration and the $\log_{10}$ NoV concentration was observed and determined statistically significant by ANOVA ($p < 0.001$). In addition, all of the interpolated data points showed 99% confidence interval (mean ± 2.58 × standard error) higher than the reference point 0, indicating successful detection over all seven orders of magnitude of NoV concentrations. Overall, this original interpolation method supports that the optimum antibody amounts must be determined for NoV detection in future sensing applications.

CONCLUSION

Rapid, simple, and sensitive method of detecting NoV antigens from water samples is demonstrated in this work that can be used towards a precautionary measure to prevent acute gastroenteritis outbreaks. While EIAs are suitable methods as a rapid detection method for NoV, they suffer inherent limitations arising from inferior sensitivity and low ELISA titer of available antibodies to NoV. Due to these limitations, most NoV EIAs are for analyzing human stool samples

from already infected subjects, whose NoV concentrations are sufficiently high (at least a few ng/mL). Other complementary methods have been attempted to overcome these limitations, but have typically made the assay substantially slower and laborious, for example, adding an additional step of PCR.[11] The innovative approach used in this work was able to demonstrate a very low detection limit (10 pg/mL) without adding additional steps. In addition, this method achieved an extremely wide linear range of assay (seven orders of magnitude), through simply using three different concentrations of anti-NoV conjugated particles. This method can also be adapted to any other virus pathogen whose antibodies are less sensitive and have low ELISA titer. Ultimately, this novel method may enhance the preventive power of EIAs towards efficient determination of contaminated water sources in order to prevent epidemics.

ACKNOWLEDGEMENTS

Ms. Jamie L. Hernandez at the University of Arizona (currently at University of Washington) assisted with running the assays; Mr. Collin A. Gilchrist at the University of Arizona assisted the fabrication of paper microfluidic chips and preparation of reagents.

DECLARATION OF CONFLICTING INTERESTS

The authors declared no potential conflicts of interest with respect to the research, authorship, and/or publication of this article.

FUNDING

Funding for this research was provided by the Water and Environmental Technology (WET) Center and BIO5 Institute at the University of Arizona, as well as Tucson Water.

REFERENCES

1. Teunis, P. F. M.; Moe, C. L.; Liu, P.; et al. Norwalk Virus: How Infectious is it? *J. Med. Virol*. **2008**, *80*, 1468-1476.
2. Yakes, B. J.; Papafragkou, E.; Conrad, S. M.; et al. Surface Plasmon Resonance Biosensor for Detection of Feline Calicivirus, a Surrogate for Norovirus. *Int. J Food Microbiol.* **2013**, *162*, 152-158.
3. Hong, S. A.; Kwon, J.; Kim, D.; et al. A Rapid, Sensitive and Selective Electrochemical Biosensor with Concanavalin A for the Preemptive Detection of Norovirus. *Biosens. Bioelectron*. **2015**, *64*, 338-344.
4. Costantini, V.; Grenz, L.; Fritzinger, A.; et al. Diagnostic Accuracy and Analytical Sensitivity of IDEIA Norovirus Assay for Routine Screening of Human Norovirus. *J. Clin. Microbio*. **2010**, *48*, 2770-2778.
5. Jones, M.K.; Watanabe, M.; Zhu, S.; et al. Enteric Bacteria Promote Human and Mouse Norovirus Infection of B Cells. *Science*. **2014**, *346*, 755-759.
6. Shigemoto, N.; Tanizawa, Y.; Matsuo, T.; et al. Clinical Evaluation of a Bioluminescent Enzyme Immunoassay for Detecting Norovirus in Fecal Specimens from Patients with Acute Gastroenteritis. *J. Med. Virol.* **2014**, *86*, 1219-1225.

7. Hurwitz, A. M.; Huang, W.; Kou, B.; et al. Identification and Characterization of Single-chain Antibodies that Specifically Bind GI Noroviruses. *PLOS ONE* **2017**, *12*, e0170162.
8. Yasuura, M.; Fujimaki, M. Detection of Extremely Low Concentrations of Biological Substances Using Near-Field Illumination. *Sci. Rep.* **2016**, *6*, 39241.
9. Ashiba, H.; Sugiyama, Y.; Wang, X.; et al. Detection of Norovirus Virus-like Particles Using a Surface Plasmon Resonance-assisted Fluoroimmunosensor Optimized for Quantum Dot Fluorescent Labels. *Biosens. Bioelectron*. **2017**, *93*, 260-266.
10. Hagström, A. E. V.; Garvey, G.; Paterson, A. S.; et al. Sensitive Detection of Norovirus Using Phage Nanoparticle Reporters in Lateral-Flow Assay. *PLoS ONE*. **2015**, *10*, e0126571.
11. Matsushita, T.; Shirasaki, N.; Tatsuki, Y.; et al. Investigating Norovirus Removal by Microfiltration, Ultrafiltration, and Precoagulation-microfiltration Processes Using Recombinant Norovirus Virus-like Particles and Real-time Immuno-PCR. *Water Res.* **2013**, *47*, 5819-5827.
12. You, D. J.; Geshell, K. J.; Yoon, J.-Y. Direct and Sensitive Detection of Foodborne Pathogens within Fresh Produce Samples Using a Field-Deployable Handheld Device. *Biosens. Bioelectron*. **2011**, *28*, 399-406.
13. Fronczek, C. F.; You, D. J.; Yoon, J.-Y. Single-pipetting Microfluidic Assay Device for Rapid Detection of Salmonella from Poultry Package. *Biosens. Bioelectron*. **2013**, *40*, 342-349.
14. Park, T. S.; Li, W.; McCracken, K. E.; et al. Smartphone Quantifies *Salmonella* from Paper Microfluidics. *Lab Chip* **2013**, *13*, 4832-4840.
15. Cho, S.; Park, T. S.; Nahapetian, T. G.; et al. Smartphone-based, Sensitive µPAD Detection of Urinary Tract Infection and Gonorrhea. *Biosens. Bioelectron.* **2015**, *74*, 601-611.

16. Nicolini, A. M.; Fronczek, C. F.; Yoon, J.-Y. Droplet-based Immunoassay on a 'Sticky' Nanofibrous Surface for Multiplexed and Dual Detection of Bacteria Using Smartphones. *Biosens. Bioelectron.* **2015**, *67*, 560-569.
17. Park, T. S.; Cho, S.; Nahapetian, T. G.; et al. Smartphone Detection of UV LED-Enhanced Particle Immunoassay on Paper Microfluidics. *SLAS Technol.* **2017**, *22*, 7-12.
18. Park, T. S.; Yoon, J.-Y. Smartphone Detection of *Escherichia coli* from Field Water Samples on Paper Microfluidics. *IEEE Sens. J.* **2015**, *15*, 1902-1907.
19. Jang, I.; Song, S. Facile and Precise Flow Control for a Paper-based Microfluidic Device through Varying Paper Permeability. *Lab Chip*. **2015**, *15*, 3405-3412.
20. Torul, H.; Ciftci, H.; Cetin, D.; et al. Paper Membrane-based SERS Platform for the Determination of Glucose in Blood Samples. *Anal. Bioanal. Chem.* **2015**, *407*, 8243-8251.
21. Kim, J.-Y.; Yeo, M.-K. A Fabricated Microfluidic Paper-based Analytical Device (μPAD) for *In Situ* Rapid Colorimetric Detection of Microorganisms in Environmental Water Samples. *Mol. Cell. Toxicol.* **2016**, *12*, 101-109.
22. StataCorp LP. *Stata/IC 12.0*. **2011**, http://www.stata.com.
23. Noel, J. S.; Frankhauser, R. L.; Ando, T.; et al. Identification of a Distinct Common Strain of "Norwalk-like Viruses" Having a Global Distribution. *J. Infect. Dis.* **2000**, *179*, 1334-1344.

FIGURES

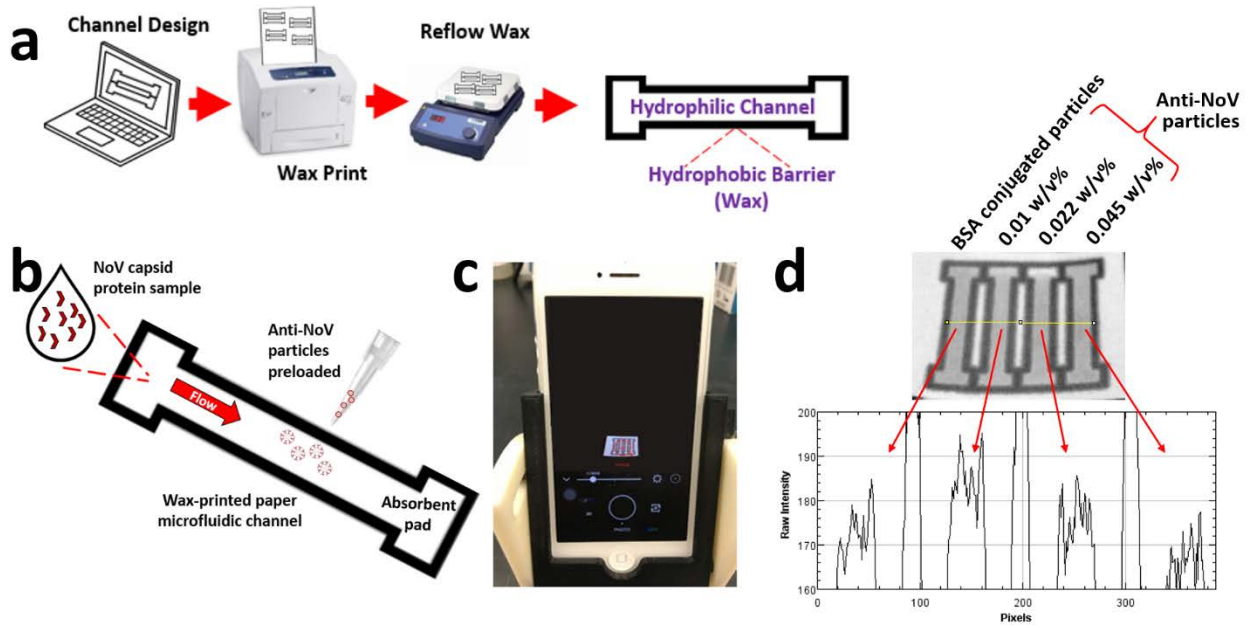

Figure 1. Assay procedure. **a)** Microchannel layouts were designed in SolidWorks and printed to chromatographic paper using a wax printer. The printed chips were placed on a hot plate to melt the wax, filling the entire depth of paper, creating hydrophobic wax barriers around the microfluidic channel. **b)** Anti-NoV conjugated particles were preloaded and dried at the center of each microfluidic channel. Sample solution containing NoV capsid proteins was loaded to the inlet of the microfluidic channel. **c)** Image of a paper microfluidic chip, acquired from smartphone app. **d)** Intensity profile across all four channels for immunoassaying 1 ng/mL NoV sample. An average raw intensity was evaluated for each channel. For this case, the intensity was maximum where 0.01 w/v% anti-NoV particles were loaded.

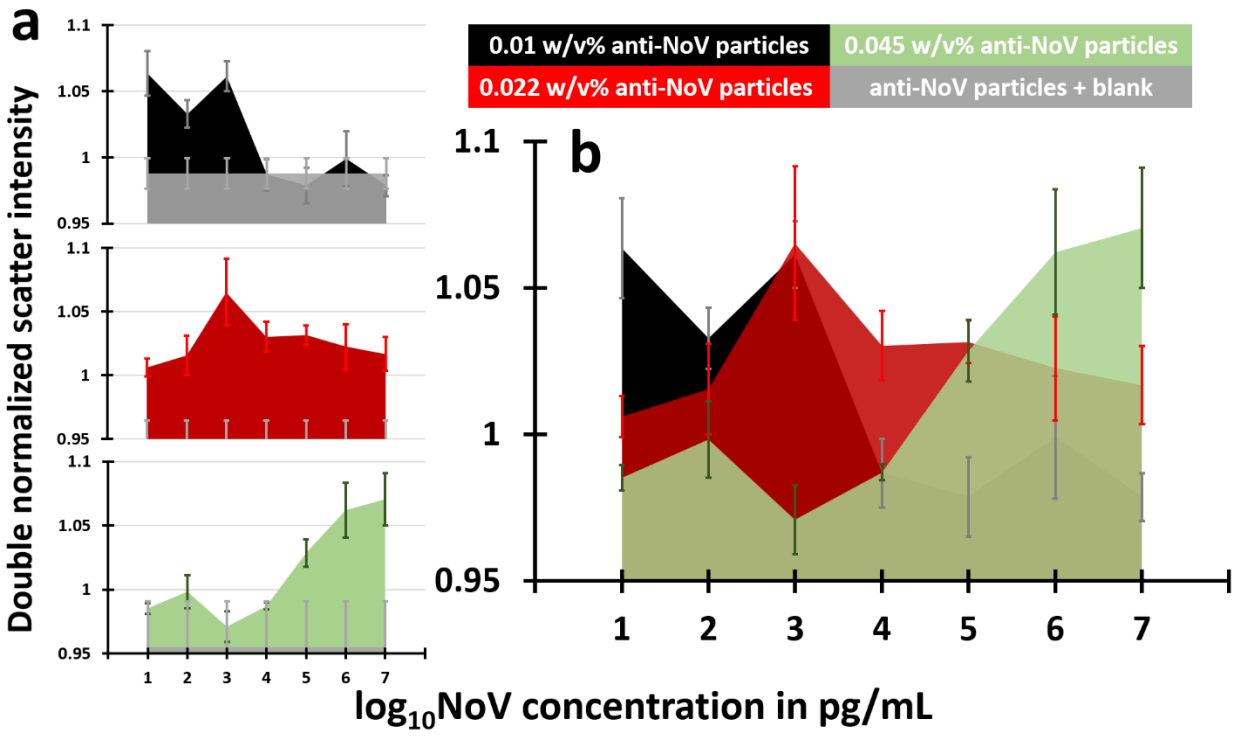

Figure 2. Results of particle immunoagglutination assay with smartphone-based Mie scatter detection from paper microfluidic chips. All data were normalized to those from a negative channel, where the same amount of BSA conjugated particles were pre-loaded. Data represents an average of three different experiments, each time using different paper microfluidic chip. Error bars represent standard errors. **a)** Double normalized scatter intensity plotted against $\log_{10}$ NoV concentration in pg/mL, using 0.01 w/v% (black), 0.022 w/v% (red), and 0.045 w/v% (green) anti-NoV conjugated particles. Blank signals are represented in grey color. **b)** All three plots were stacked together.

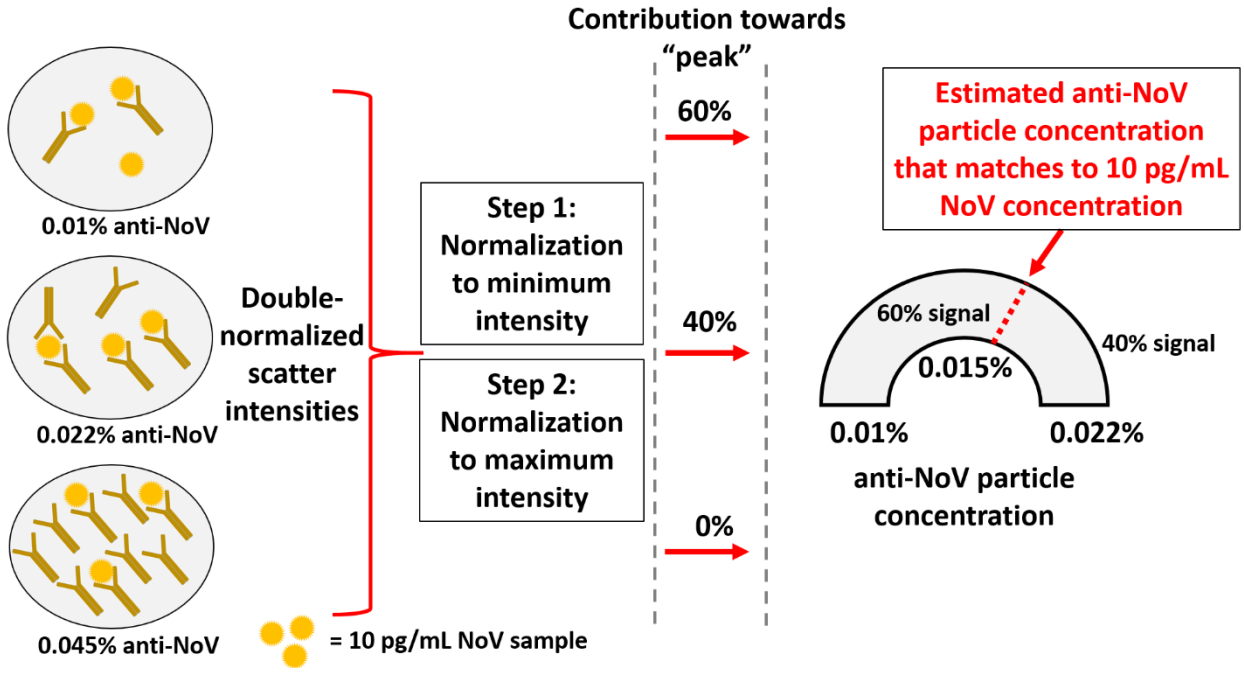

Figure 3. Graphical illustration for estimating the interpolated value of anti-NoV particle concentration for the given NoV concentration (in this case, 10 pg/mL).

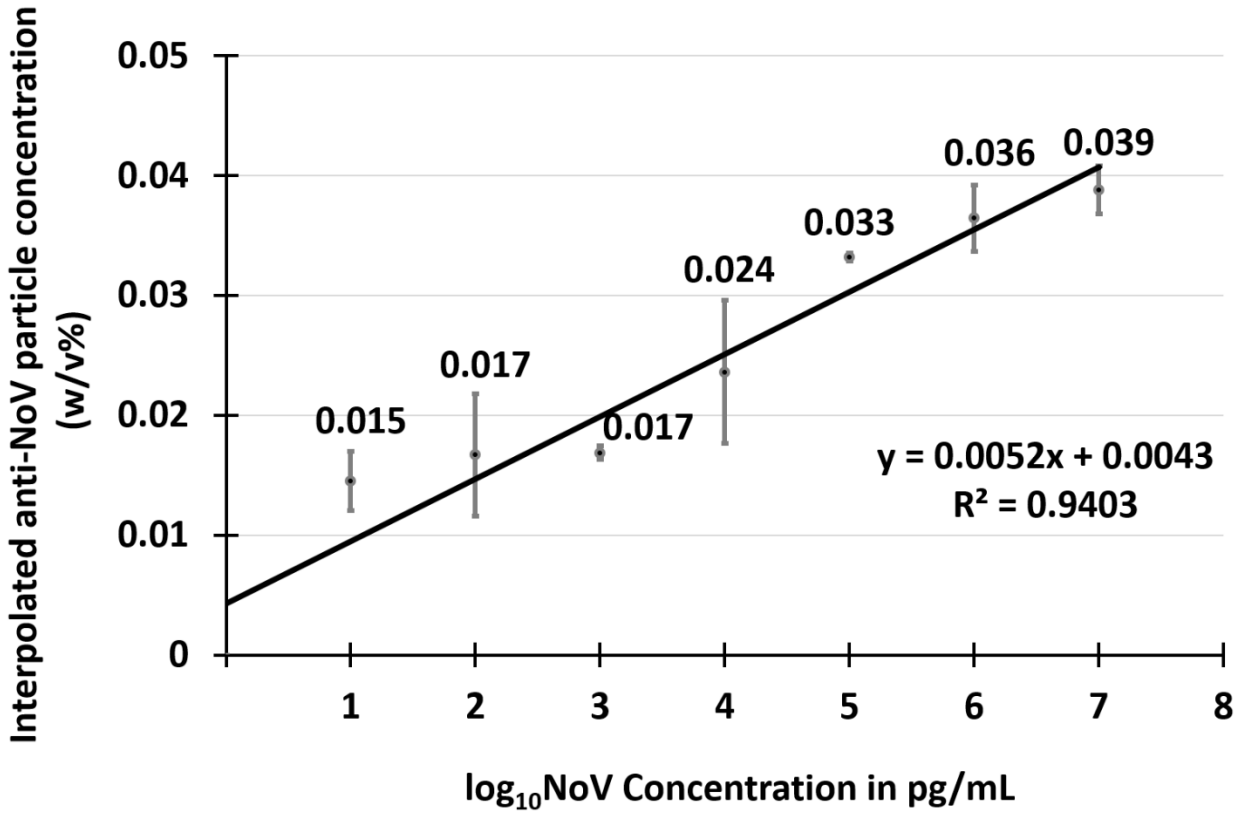

Figure 4. The interpolated anti-NoV particle concentrations were plotted against $\log_{10}$ NoV concentration in pg/mL. Each data point was obtained from 9 different experiments (three different anti-NoV particle concentration, each replicated three times). Error bars represent standard errors. The 99% confidence intervals (mean ± 2.58 × standard error) for all data points were higher than 0, indicating all data points are statistically different from the blank with 99% confidence.